Reversal Modes, Thermal Stability and Exchange Length in Perpendicular Recording Media

Dieter Suess, Thomas Schrefl, and Josef Fidler

***Abstract*—Micromagnetic simulations are performed to investigate the reversal process and the thermal stability of a grain of a typical perpendicular recording media (Co–Cr). The integration of the LLG equation yields that the reversal process changes slowly and steadily from coherent rotation to nucleation with increasing column length. The region between homogeneous rotation and nucleation becomes smaller and is shifted to smaller column lengths if the damping constant is reduced from $\alpha = 1$ to $\alpha = 0.02$. In the weakly damped case very fast switching modes exist if the switching field is only slightly larger than the coercive field. In this small regime the switching time increases with higher switching fields. Using solutions of LLG simulations, energy barriers between the two stable states at zero field are estimated. For column lengths larger than 30 nm the energy barrier for inhomogeneous reversal processes are smaller than for coherent rotation.**

***Index Terms*—Energy barriers, fast switching, micromagnetics, perpendicular recording, thermal stability.**

I. Introduction

IN RECENT years there has been a renewed interest in perpendicular recording since an improvement of the areal density in longitudinal recording is getting increasingly difficult. The main advantage of perpendicular recording is that the areal density can be increased without reducing the volume of the magnetic bit. A large volume of the magnetic domain can be realized with an increased column length l_c (film thickness). For coherent rotation a higher grain volume leads to a higher energy barrier and hence to an improved thermal stability. Thus twice the exchange length $2R_0$, which is assumed to be the limit between coherent rotation and inhomogeneous reversal processes, is the upper bound for the column length in perpendicular recording media [1]. For Co–Cr, a typical perpendicular recording material, $2R_0 = (2/M_s)\sqrt{4\pi A/\mu_0} \approx 50$ nm.

We have performed micromagnetic simulations to investigate in detail the reversal modes in perpendicular recording media. The simulations are based on the integration of the LLG equation. Details about the method can be found in [2]. The energy barrier between two stable magnetization states is estimated from LLG solutions.

Manuscript received October 13, 2000.

This work was supported by the Austrian Science Fund (P13260 and Y132-PHY).

D. Suess is with the Institute of Applied and Technical Physics, Vienna University of Technology, Wiedner Hauptstr. 8-10, A-1040 Vienna, Austria (e-mail: suess@magnet.atp.tuwien.ac.at).

T. Schrefl (e-mail: thomas.schrefl@tuwien.ac.at).

J. Fidler (e-mail: fidler@email.tuwien.ac.at).

Publisher Item Identifier S 0018-9464(01)07298-3.

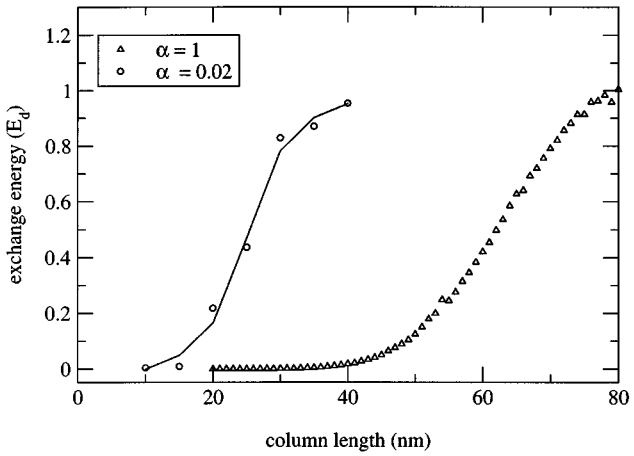

Fig. 1. Maximum value of the exchange energy during reversal as a function of the column length for two different damping constants. A value of the exchange energy close to the domain wall energy $E_{\rm d}$ indicates that nucleation processes occurs at the particle ends.

II. Model and Results

We have calculated the reversal process in one Co-Cr grain ($J_s = 0.5$ T, $A = 10^{-11}$ J/m, $K_1 = 3 \times 10^5$ J/m^3). The basal plane of the grain is an irregular pentagon with a diameter of about 12 nm (Fig. 2). The easy axis is perpendicular to the basal plane and parallel to the z-axis. For all calculations presented in the paper the external field is applied 1° off the easy axis. The average element size of the finite element mesh is 2 nm, small enough to resolve domain walls which have a typical width of $d_w = \sqrt{A/K_1} = 6$ nm.

A. High Damping Reversal ($\alpha = 1$)

If the external field reaches the coercive field H_c, which increases linearly from $0.97\ (2K_1/J_s)$ for $l_c = 20$ nm to $1.03\ (2K_1/J_s)$ for $l_c = 70$ nm, the magnetization state becomes unstable and reversal starts. Fig. 1 shows the maximum value of the exchange energy during reversal for different column lengths. The exchange energy measures the uniformity of the magnetization during reversal. The exchange energy is normalized with the domain wall energy $E_w = 4A_{\rm end}\sqrt{AK_1}$. $A_{\rm end}$ measures the area of the basal plane. It can be seen that nucleation does not occur at a critical length, but the transition is smooth from coherent rotation to nucleation. Below 40 nm coherent rotation dominates. Fig. 2 shows nonequilibrium states of the magnetization during reversal for different column lengths at a time when $J_z = 0$. With increasing column length $(> 40$ nm$)$ the magnetization at the top and bottom of the grain

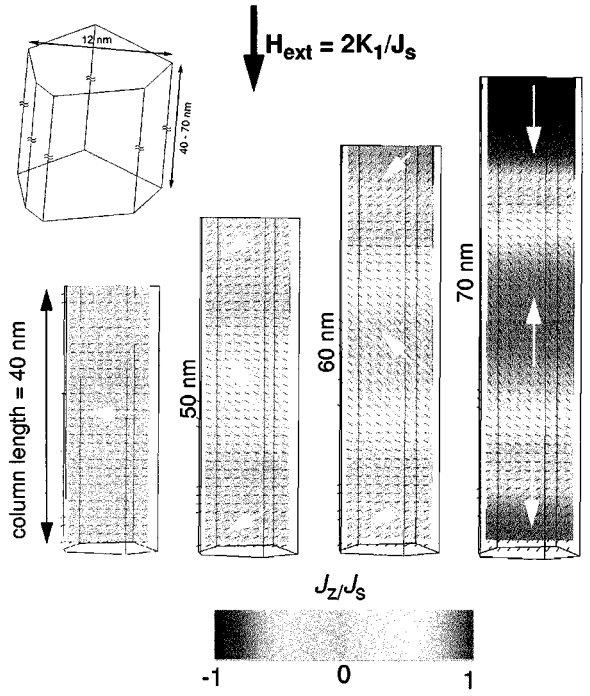

Fig. 2. Non-equilibrium states ($J_z = 0$) during reversal for different column lengths after the coercive field was applied. ($\alpha = 1$) The inset top left shows the geometry of the columnar grain.

becomes increasingly misaligned to the magnetization in the middle. Above 80 nm the magnetization at the top and bottom points antiparallel to the magnetization in the middle and the magnetic exchange energy reaches its maximum. In this regime on both ends domain walls are formed. The maximal exchange energy during reversal is equal to the domain wall energy E_w.

B. Low Damping Reversal ($\alpha = 0.02$)

The transition from coherent rotation to nucleation becomes different when a damping constant $\alpha = 0.02$ is assumed. The magnetization becomes incoherent during reversal for $l_c \geq 20$ nm. For $l_c = 20$ nm the reversal process starts with homogeneous rotation. When J_z/J_s becomes smaller than ~ 0.2, the high strayfield due to magnetic charges at the surfaces normal to the basal plane, forms a flower state. This flowerstate transforms to a homogeneous state again, when J_z/J_s becomes smaller than ~ -0.2.

C. Switching Times

To calculate the switching time an external field larger than the coercive field is applied instantaneously to the saturated state. Thus we look at the dynamic response of the system for fixed external field with the saturated state as initial configuration. Fig. 3 shows the time until J_z/J_s becomes smaller than -0.5 as a function of the strength of the external field. The column length of the grain is 20 nm ($\alpha = 0.02$). It is conspicuous that the switching time does not decrease with increasing external field in the whole regime but shows a maximum slightly above the coercive field. We found this dependence also for a single spin under the action of an external field, provided the uniaxial easy axis is not aligned exactly parallel to the applied field. Fig. 4 shows the time dependence of the magnetization

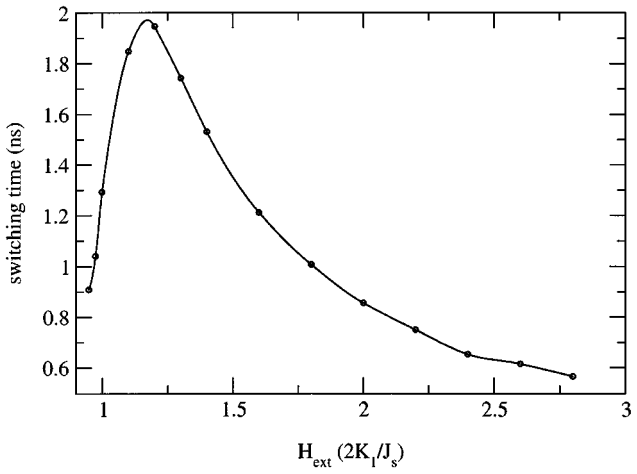

Fig. 3. The switching time, which measures the time until J_z reaches -0.5 after applying an external field in z-direction to the saturated state, as a function of the strength of the external fields. The easy axis is one degree misaligned from the z-axis. ($\alpha = 0.02$).

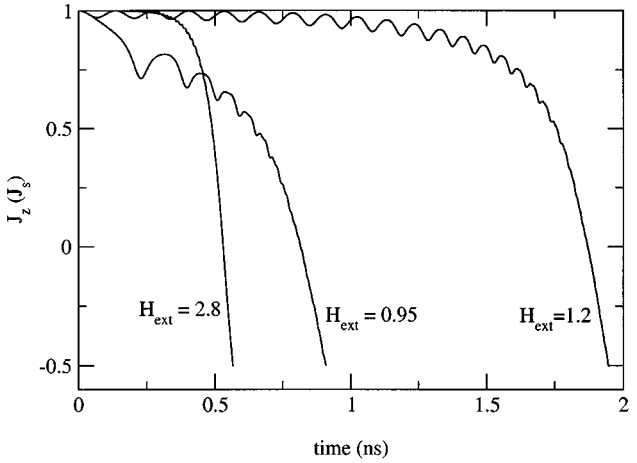

Fig. 4. J_z as a functions of time after different external fields (0.95, 1.2 and 2.8 times $2K_1/J_s$) are instantaneously applied to the saturated state. The column length of the grain is 20 nm. ($\alpha = 0.02$).

for different strengths of the external field. At $t = 0$ a field of 0.95, 1.2 and 2.8 ($2K_1/J_s$) is applied. For small values of the external field the z-component does not decrease monotonically but shows oscillations, which correspond to the precession of the magnetization around the effective field. This effect can only be found if the axial symmetry is broken (easy axis does not point exactly parallel to field direction) and an increase of J_z does not necessarily lead to an increase of the energy. With increasing damping constant the relaxation toward the minimum dominates the motion of the magnetization and the oscillations of the magnetization vanish for every strength of the external field.

To explain why the switching becomes faster with decreasing external field we have investigated the curvature of the energy landscape for a single spin under the action of an external field in z-direction. The uniaxial easy axis is one degree misaligned to the z-axis. If J_z is restricted to be larger than zero, the energy landscape can be drawn as a function of J_x and J_y. If the external field is slightly larger than the coercive field the energy landscape near the initial state (saturated state) shows

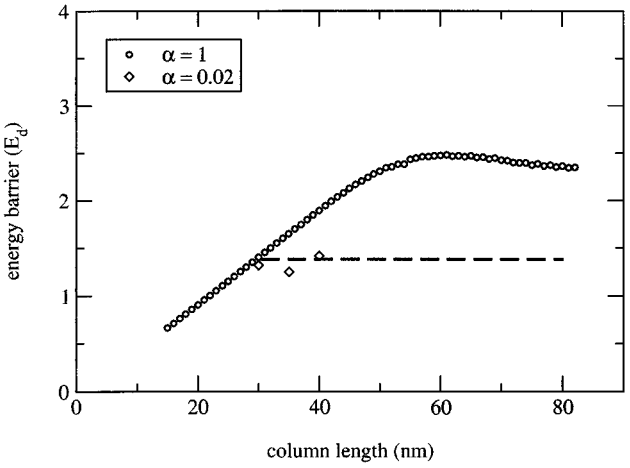

Fig. 5. Upper limit of the energy barrier as a function of the column length. For l_c larger than 30 nm the estimation of the upper limit on the basis of LLG simulation with $\alpha = 0.02$ leads to smaller energy barriers (diamonds).

a plateau. The path in configuration space with the same energy passing the initial state is relatively long. The precession term in the LLG equation moves the magnetization along this path, if α is small. Hence states far away from the initial state which correspond to large values of $\sqrt{J_x^2 + J_y^2}$ can be reached. These states correspond to local minima of J_z in Fig. 4. In these states a high torque $(\alpha\gamma'/J_s)\mathbf{J} \times (\mathbf{J} \times \mathbf{H})$ acts on the magnetization. This torque follows from the Landau–Lifshitz equation and reaches a maximum value when $J_z = 0$. The high torque is responsible for the fast relaxation toward the reversed state. If a large external field is applied it dominates the effective field. Hence the magnetization precesses around the z-axis with a small value of $\sqrt{J_x^2 + J_y^2}$. The torque remains small for a longer time which leads to higher switching times. Only for fields exceeding 1.2 times the anisotropy field the switching time decreases. This is due to the linear increase of the torque with the strength of the external field.

D. Energy Barriers

To estimate the energy barrier between the two stable states (magnetization up and down) for vanishing external field we assume that the reversal process at zero temperature triggered by the external field is similar to the reversal process at zero field and finite temperature. Hysteresis loop calculations using the LLG equation provide the magnetization states during reversal. This path in configuration space is one possible path from the saturated state toward the reversed state, also at zero field. The calculation of the energy along this path, assuming zero field, yields the energy landscape for this path. Because this particular path does not necessarily pass through the saddle point, we can only determine an upper limit for the energy barrier. On the basis of such a path the elastic band method can be used to find the saddle point [3].

We use two different paths in configuration space to find upper limits for the energy barrier. The first path is obtained from a calculation with $\alpha = 1$. The second path describes the reversal process for $\alpha = 0.02$. The path corresponding to $\alpha = 0.02$ contains inhomogeneous states when the column length exceeds 20 nm (Fig. 1).

For column lengths smaller than 30 nm, both calculations yield the same energy barrier which increases with the column length linearly as predicted by Stoner–Wohlfarth theory (Fig. 5). When the column length exceeds 30 nm, the path corresponding to $\alpha = 0.02$ leads to smaller energy barriers. This proves that at least for column length $l_c \geq 30$ nm inhomogeneous reversal processes have a lower energy barrier than homogenous rotation.

Braun [4] calculated the energy for nucleation at the end of a wire, with a diameter $d < \sqrt{AK_1}$ or $K_1 \geq J_s^2/4\,\mu_0$ as $E_n = 4A_{\text{end}}\sqrt{A(K_1 + J_s^2/4\,\mu_0)}$.

The circles in Fig. 5 for $l_c \geq 50$ nm represent upper limits for energy barriers which are more than twice as large as the prediction by Braun [4]. The reason is that the reversal process at $T = 0$, which is used as trial path in configuration space, is symmetric for $\alpha = 1$. Hence nucleations occur on both ends and its energy is counted twice. Simulations with $\alpha = 0.02$ at $T = 0$ show only one nucleation at the particle end. Therefore energy barrier estimations on the basis of these simulations yield much smaller values (diamondes and the extrapolated dotted line in Fig. 5).

III. Conclusions

The exchange length is insufficient to determine the reversal mode. For fixed exchange constant, anisotropy constant and geometry the reversal mode may change depending on the damping constant. The switching time decreases with smaller magnitude of the external field if the field is smaller than a critical value.

References

[1] H. J. Richter, "Recent advances in the recording physics of thin-film media," *J. Phys. D: Appl. Phys.*, vol. 32, pp. 147–168, Aug. 1999.

[2] J. Fidler and T. Schrefl, "Micromagnetic modeling-the current state of the art," *J. Phys. D*, vol. 33, no. 15, pp. 135–156, 2000.

[3] G. Mills and H. Jónson, "Quantum and thermal effects in H_2 dissociative adsorption: evaluation of free energy barriers in multidimensional quantum systems," *Phys. Rev. Lett.*, vol. 72, no. 7, pp. 1124–1127, Feb. 1994.

[4] H. B. Braun, "Nucleation in ferromagnetic nanowires-magnetostatics and topology," *J. Appl. Phys.*, vol. 85, pp. 6172–6174, Apr. 1999.